^{52}Cr(p,n)^{52}Mn^{g,m} and ^{52}Cr(d,2n)^{52}Mn^{g,m} excitation functions

H. I. West, Jr., R. G. Lanier, and M. G. Mustafa
Nuclear Chemistry Division, Lawrence Livermore National Laboratory, University of California, Livermore, California 94550
(Received 24 November 1986)

We have irradiated natural chromium with protons and deuterons to produce ^{52}Mn^{g,m}, primarily from the ^{52}Cr(p,n) and ^{52}Cr(d,2n) reactions. The excitation functions up to 27 MeV were measured by the foil activation method and were compared with results from a statistical model calculation based on the Hauser-Feshbach formalism with preequilibrium emission. For ^{52}Cr(p,n)^{52}Mn^{g,m}, both the total cross section, $\sigma(g+m)$, and the isomer ratio, $\sigma(m)/\sigma(g)$, are reproduced to within 10% by the calculations. By contrast, for the ^{52}Cr(d,2n)^{52}Mn^{g,m} reaction, we find that calculations overestimate $\sigma(g+m)$ by $\sim$50% and underestimate $\sigma(m)/\sigma(g)$ by nearly one-half. We find that arbitrary adjustments of level density or preequilibrium parameters can yield approximate agreement for $\sigma(g+m)$ but do not improve the agreement for $\sigma(m)/\sigma(g)$. A part of this discrepancy may be due to the fact that the preequilibrium calculations do not include angular momentum. However, to fully understand this discrepancy, deuteron breakup effects in the entrance channel must be taken into account. A companion paper explores this idea.

I. INTRODUCTION

We have irradiated natural chromium targets with protons (6–27 MeV) and deuterons (8–20 MeV) to produce ^{52}Mn^{m} (21.0 min, $I^{\pi}=2^{+}$) and ^{52}Mn^{g} (5.6 d, $I^{\pi}=6^{+}$). The primary production processes for these products are the ^{52}Cr(p,n) and (d,2n) reactions. Only above 15 MeV does the ^{53}Cr(p,2n) reaction become significant, and ^{53}Cr(d,3n) becomes significant above 20 MeV.

Some earlier results for protons and deuterons on chromium are available. Boehm *et al.*[1] have made (p,n) cross section measurements of the ^{52}Mn^{g,m} isomeric pair from near threshold (5.60 MeV) to 6.8 MeV. Linder and James[2] made measurements from 6 to 16 MeV, Wing and Huizenga[3] from $\sim$6 to 10.5 MeV, and Tanaka and Furukawa[4] from $\sim$6 to 14 MeV. For the (d,2n) reactions we note the early measurements of Burgus *et al.*,[5] while Cogneau *et al.*[6] provided more recent data for $\sigma(m)$ and $\sigma(g)$. We make comparisons between these data and the result of our measurements in Sec. III.

Accurate measurements of the ground and isomeric state excitation functions obtained using different projectiles can be particularly useful in testing the physics involved in a statistical model calculation. Working with total cross sections, $\sigma(g+m)$, and isomer ratios, $\sigma(m)/\sigma(g)$, we have sufficient information to limit the degrees of freedom in the statistical reaction modeling. Uncertainties will usually be present in the level-density formalism, in the various final-state discrete-level configurations, in the compound-state spin distribution, and, finally, in the details of the preequilibrium processes. Some clues as to the relative importance of these effects on modeling a particular set of reactions can be sorted out by populating identical final states by different reaction channels. In particular, as in the present study, a careful statistical model calculation which attempts to reproduce the observed isomer ratios can show that the reaction process is only partially characterized by a statistical formalism and that other processes (e.g., direct reactions) must be examined. In Sec. IV we compare our experimental results with those from a statistical model analysis [based on the Hauser-Feshbach formalism with preequilibrium (PE) emission using the STAPRE (Ref. 7) computer code] and point out a significant problem involving the (d,2n) reaction. Although we note that the PE calculation does not include angular momentum, we believe that the solution to the problem lies elsewhere.

Finally, we note that this study is part of a larger experimental effort in our laboratory motivated by our interest in establishing the predictive limits of statistical model calculations in the $A\sim50$ and ~90 regions for proton, deuteron, and triton projectiles. A summary of the present work was reported previously by Mustafa *et al.*[8]

II. EXPERIMENTAL METHOD

We have used the foil activation method to obtain excitation functions for ^{52}Mn^{g,m}. This method, although relatively simple, allows one to be very specific about the reaction studied because the resultant nucleus is identified by its characteristic decay. Used properly, this method is capable of producing results of considerable accuracy. Facets of this work requiring special attention are as follows: the accelerator beam energy must be well known, the integral of the beam current must be measured accurately, and the areal density of the target must be well known, i.e., we must know

$$\int \rho(x,y,z)i(y,z,t)dx\,dy\,dz\,dt$$

accurately, where $i(y,z,t)$ is the beam current per unit area as a function of time, $\rho(x,y,z)$ the density, dx the foil thickness, $dy\,dz$ the differential of area, and dt the differential of time. The resultant activity (in this case, γ rays) must be measured with care. Finally, a correct de-

 ©1987 The American Physical Society

cay scheme must be available with the γ-ray intensities and β-decay branchings known accurately.

The Lawrence Livermore National Laboratory (LLNL) Cyclograaff was used to produce protons (0—27 MeV) and deuterons (0—20 MeV) for irradiating our targets. This accelerator uses a negative-ion fixed-energy cyclotron to inject a tandem Van de Graaff accelerator and, in this mode, produces energies above 12 MeV. Our target chamber was located in the beam line coming directly from the accelerator. Prior to each irradiation the beam energy was set by bending the beam 90° through an accurately calibrated analyzing magnet (the central field was set by a NMR signal) and a measure of the terminal voltage, i.e., a reference signal, was determined by a generating volt meter (GVM). The GVM then provided the feedback signal needed to stabilize the terminal voltage during the course of an irradiation.

The irradiation chamber (Fig. 1) was designed carefully. The beam was defined by a 10 mm hole through a 1 mm tantalum plate just upstream from the chamber. The chamber was electrically isolated, thus becoming a Faraday cup. At its entrance, an aluminum collimator (16 mm diam hole) was operated at -300 V to prevent electrons upstream from entering the chamber and those produced in the chamber, from δ-ray wall interactions, from escaping the chamber upstream. Just in front of the foil stack, small magnets ($\sim$600 G) were used to prevent δ rays (maximum energy of $4E_p m_e/m_p$) from moving upstream. The target-foil assembly and beam stop were cooled by air flowing through a cooling jacket. The integration of the beam current was determined by an ORTEC model 439 digital current integrator. The unit has a precision of 0.01% and an absolute accuracy of 0.2%. Typical beam currents were 1 μA. As a check on our procedures, we measured several points near the peak of the excitation function for the well-known ^{65}Cu(p,n)^{65}Zn reaction.[9] Our measured values were well within quoted errors.

Our targets were of natural chromium, which consists of ^{50}Cr (4.345%), ^{52}Cr (83.789%), ^{53}Cr (9.501%), and ^{54}Cr (2.365%). The target foils were made by the Materials Fabrication Division of LLNL, by evaporating chromium on to 2.5 cm diam, 25 μm thick aluminum foils to a thickness of 1.2—6.0 mg/cm^2. For thicknesses greater than 1.3 mg/cm^2, the chromium was evaporated on both sides to prevent curling of the backing foil. During the course of the evaporation, the fixture holding the aluminum foils was oscillated to ensure a uniform coat of chromium over the surface of the foils. Although we made studies using x-ray fluorescent techniques, it is difficult to get a realistic measure of the uniformity of the foils except through the reproducibility of comparative measurements. The beam hitting the foil was 3—10 mm in diameter and small irregularities were averaged out. From a number of similar measurements, we estimate that any uncertainties due to density gradients on the foils was no more than $\pm 2\%$.

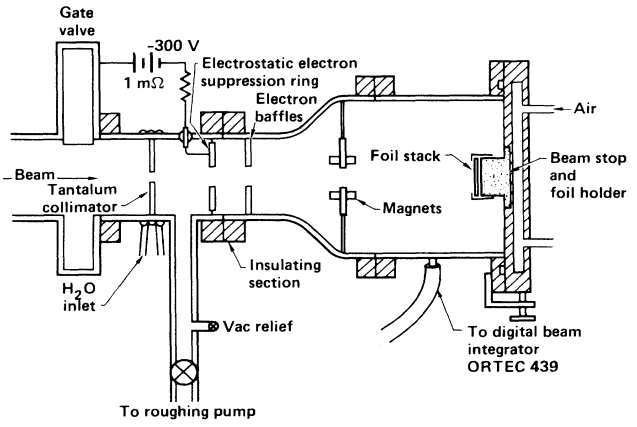

FIG. 1. Irradiation chamber. The straight sections are accelerator beam-line sections.

Normally in our foil work, two or more foils are used. A 25-μm aluminum foil, just behind the target foil, is used to catch ions recoiling out of the primary foil, and their count gives a measure of momentum transfer during the reaction. Other aluminum foils are used as needed to further degrade the beam energy between foils. In those cases where we obtained both metastable and ground state data, a single chromium foil with aluminum catcher foil was used. We first irradiated for 1.0—2.0 min (60—120 μC) and counted the 1434-keV gamma ray from the decay of the 21.0-min isomer (see Fig. 2 with data from Lederer *et al.*[10]). This operation consisted of a 10.0-min wait after irradiation (to reduce the effects of short-lived activities) followed by four 10.0-min counts using a large-volume germanium detector located near the accelerator. The foils were then returned to the accelerator to obtain a total bombardment of 1000—4000 μC. The foils were counted four times on accurately calibrated germanium detectors[11] and the results analyzed by the code GAMANAL.[12] All three γ rays listed in Fig. 2 were used in this part of the cross section measurements, which helped minimize statistical fluctuations. Representative foils from this counting were then used to cross calibrate the detector used for the isomer measurements.

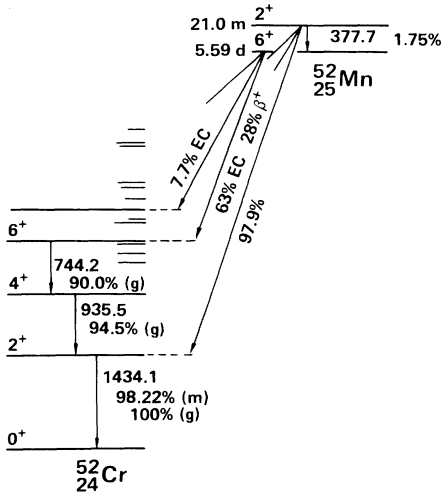

FIG. 2. Decay scheme for ^{52}Mn^{g,m}. Results are from the Nuclear Data Tables [Lederer *et al.* (Ref. 10)]. Our measurement confirms the γ-ray intensities I_γ with accuracy and are consistent with the 28% β^+ branch. (g) refers to ground state decay, (m) to metastable decay. Energies are in keV.

The gamma rays in the nuclear decay have an appreciable probability of coincidence summing in the detector. We note that a photopeak count can be lost by any interaction in the detector produced by the other gamma rays in the cascade, by x rays, or by annihilation of positrons—showing up through Compton or photoelectric interaction. X rays were eliminated by use of a 1.275 g/cm^2 aluminum absorber which also localized the annihilation of the positrons to a defined region. Because of the coincidence summing, it was necessary to make corrections that amounted to as much as 3%. The final error assigned to the counting data consists of ±2.0% calibration uncertainty[11] and counting statistics. The latter were usually $<1\%$.

The decay scheme used for interpreting the data is shown in Fig. 2 and comes from Lederer *et al.*[10] The relative intensities for the 744.2-, 935.5-, and 1434.06-keV gamma rays are consistent with measurements from our detectors. Note the 28% β^+ intensity for the ^{52}Mn^g decay. Some experimenters in the past have used 35% in the interpretation of beta-counter data, which gives a different value for their cross sections compared to ours. When it was evident that this was a problem, we made corrections before making the data comparisons. We had some concern about the lifetime of the isomer. R. Nagle of our laboratory remeasured the value, obtaining 21.0±0.04 min, which is in good agreement with that in Lederer *et al.*[10]

III. EXPERIMENTAL RESULTS

The $^{52+x}$Cr(p,n, + xn)^{52}Mn^{g,m} excitation functions are given in Table I and Figs. 3 and 4. The ground-state threshold for the (p,n) reaction is $E_{lab}=5.60$ MeV. Above $E_{lab}=13.69$ MeV, the data have a small contribution from the (p,2n) reaction. Calculations show that at 20—25 MeV, the contribution is ~30 mb (see Fig. 8). The (p,3n) reaction has a threshold of 23.58 MeV, but makes an insignificant contribution to the results.

The first column in Table I gives the average particle energy in the foils. The second column gives the apparent cross section $\sigma(ga)$ for populating the ground state of ^{52}Mn. The third column gives the true ground state cross section. The fourth column gives the cross section for populating the 21.0-min isomer. Note that $\sigma(ga)$ and $\sigma(m)$ are the results of dividing the respective counting rates by the I_γ's in Fig. 2. In Sec. III A we discuss correcting $\sigma(ga)$ for decay from the isomeric state to give $\sigma(g)$.

Double-sided foils were used for the proton work. In the rising portion of the excitation function, the energy change in the beam between entering the first chromium foil and exiting the second foil was typically 0.35 MeV. With an energy loss in each chromium foil of ~0.07 MeV, we then had two contributions to a given measurement, one centered at $E_{lab}+(0.35/2)-0.035$ and the second at $E_{lab}-(0.35/2)+0.035$ MeV. A small code was written to correct for energy variations over a foil thickness, which in this case meant that we calculated the average energy by determining the energy loss in the two chromium foils separated by the energy loss in the aluminum mounting foil. As long as the cross section, written as a power series in E, $\sigma(E)=a+bE+cE^2+dE^3$, is adequately represented by the first two terms on the right (which was fitted to the data by the methods of least squares), no correction to the average energy is required. In the rising portion of the excitation function, c, and higher order terms, were significant.

TABLE I. The $^{52+x}$Cr(p,n + xn)^{52}Mn^{g,m} excitation function.[a]

E_{lab} (MeV)	$\sigma(ga)$[c] (mb)	$\sigma(g)$[d] (mb)	$\sigma(m)$[c] (mb)
6.30[b]	4.44	2.86	89.8
6.75[b]	14.14	10.68	196.5
7.32	26.0	22.3	211.1
7.79	41.1	36.9	236.8
8.78	56.9	51.7	294.9
9.84	80.9	74.8	344.2
11.82	111.7	105.4	356.3
14.24	138.2	132.7	311.6
15.39	120.7	116.4	243.8
16.89	96.1	92.9	181.9
18.90	61.1	59.5	89.9
20.91	44.4	43.3	62.5
22.91	35.7	34.8	48.9
24.91	29.1	28.4	40.0
26.91	24.6	24.0	34.3

[a]The threshold for the (p,2n) reaction is 13.69 MeV. The contribution to the total at 24—26 MeV is ~30 mb.
[b]Corrections were made to allow for nonlinear variation of the cross section over the range of particle energy variation in the foils (see text).
[c]These measurements are σ(natural)/abundance of ^{52}Cr (0.8379). The relative accuracy in σ is ±2%. For absolute accuracy use ±3%. This is the apparent cross section (see text).
[d]The true cross section, $\sigma(g)$, results from correcting $\sigma(ga)$ for decay from the metastable state.

To obtain the correction we proceeded as follows: The activity produced in a foil of thickness dx is proportional to σdx or $\sigma(dE/dx)^{-1}dE$. But the variation of dE/dx over a foil thickness is usually negligible, so that it is sufficient to use only $\sigma(E)dE$. The average cross section is then $\sigma_{av}=(1/\Delta E)\int\sigma(E)dE$, where ΔE is the mean energy loss in the foil. Our coding was set up to include straggling, but this had a minor effect on the result. Our experimental result, σ_{expt}, is equivalent to σ_{av}, except that σ_{av} reflects the least squares fit. We thus normalized the fit in the region of interest to $\sigma_{expt}/\sigma_{av}$ and read the corrected cross section from the polynomial fit at E_{av}. Only the two lowest points for the (p,n) data required a correction; e.g., the point at 6.30 MeV went from 4.85 to 4.44 mb. Note that the correction does not result in smoothing the data. In the mode in which we were using the Cyclograaff, the energy variation was ±0.01 MeV for $E\leq 12$ MeV (Van de Graaff only) and ±0.020 MeV above that energy. However, from analysis of data obtained in the rising portion of the excitation function, we find that we should probably use ±0.020 MeV as an estimate of the accuracy at all energies.

Table II and Figs. 5 and 6 give the excitation function for ^{52}Cr(d,2n)^{52}Mn^{g,m}. The energies are given in column 1

in Table II. Unlike the proton work, single-sided foils were used for energies up to 11.47 MeV, minimizing the energy correction. Column 2 gives the apparent ground-state cross sections, column 3 the corrected ground-state cross sections, and column 4 the isomer cross sections. The earlier comments regarding errors, etc. pertain. There is some competition from deuteron reactions with other isotopes present in the target. The ^{53}Cr(d,3n) reaction has a ground-state threshold of 16.25 MeV. From the ALICE code[13] we estimate a contribution of ~ 5 mb at 20 MeV which is of the order of the error in the measurements, and thus we have made no corrections to the data.

A. Isomer ratios

Figure 7 is a plot of the ratio $\sigma(m)/\sigma(g)$. Note in Fig. 2 that the 2^+ isomeric state of ^{52}Mn has a weak 1.75% decay branch to the 6^+ ground state. To obtain the true value of $\sigma(g)$ we must make a correction for this branch which becomes quite significant when $\sigma(m) > \sigma(g)$. The correction is given by

$$\sigma(g) = \sigma(ga) - [f\lambda_m/(\lambda_m - \lambda_g)]\sigma(m)$$
$$= \sigma(ga) - 0.0176\sigma(m) .$$

Here, f equals the decay branch, and λ_m and λ_g are the respective decay constants. The corrected values are given in Tables I and II. The effect of the correction in the (p,n) data makes a marked change in $\sigma(m)/\sigma(g)$ at low energies.

We note the marked dissimilarity between the isomer ratios obtained for the proton data and that obtained for the deuteron data. Figure 7 shows the results from using the STAPRE code to model the ratios. The results are discussed later.

B. Data comparisons

Data, available in the literature, have been examined and comparisons are made in Figs. 3—6. There is no evidence that the authors corrected $\sigma(g)$ for feeding from the isomeric state; therefore, in our comparisons we use $\sigma(ga)$. Wing and Huizenga[3] have made measurements for ^{52}Cr(p,n)^{52}Mn^{g,m} from 6 to 10.5 MeV. Their experimental procedure was much like ours, except that they used a carefully calibrated scintillation counter and counted only the photopeak of the 1434-keV γ ray. The agreement with our data for both ^{52}Mn^g and ^{52}Mn^m is within experimental accuracy, as can be seen from Fig. 3. They consider the error in cross section to be less than 10%. The uncertainty in proton energy at 10 MeV was about 0.15 MeV, increasing to about 0.56 MeV at 5 MeV.

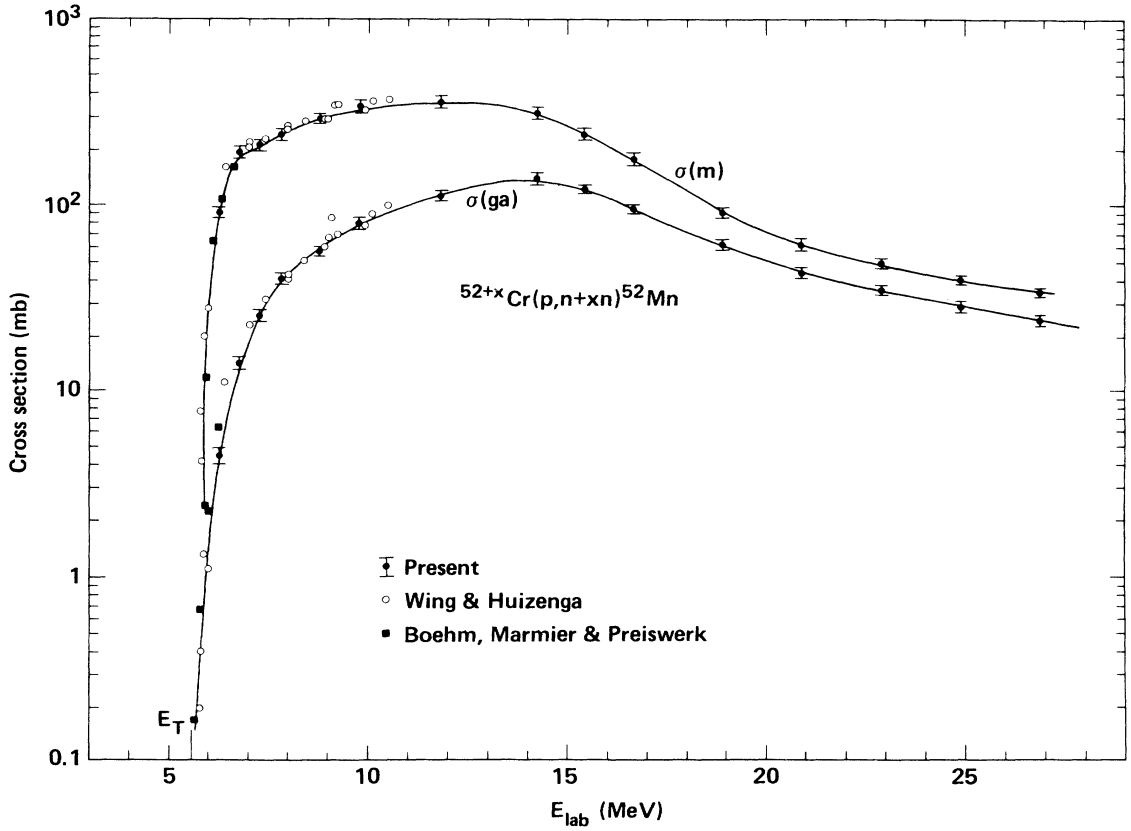

FIG. 3. The $\sigma(ga)$ and $\sigma(m)$ cross section for $^{52+x}$Cr(p,n + xn)^{52}Mn. A contribution from the (p,2n) reaction begins at 13.69 MeV. Note that $\sigma(ga)$ is the apparent ground state cross sections (see Sec. III A) and near threshold can be considerably larger than $\sigma(g)$. Earlier measurements are shown for comparison. Wing and Huizenga consider the uncertainties in their data to be less than 10%. See the text for discussion of the comparison with the data of Boehm *et al.* (Ref. 1).

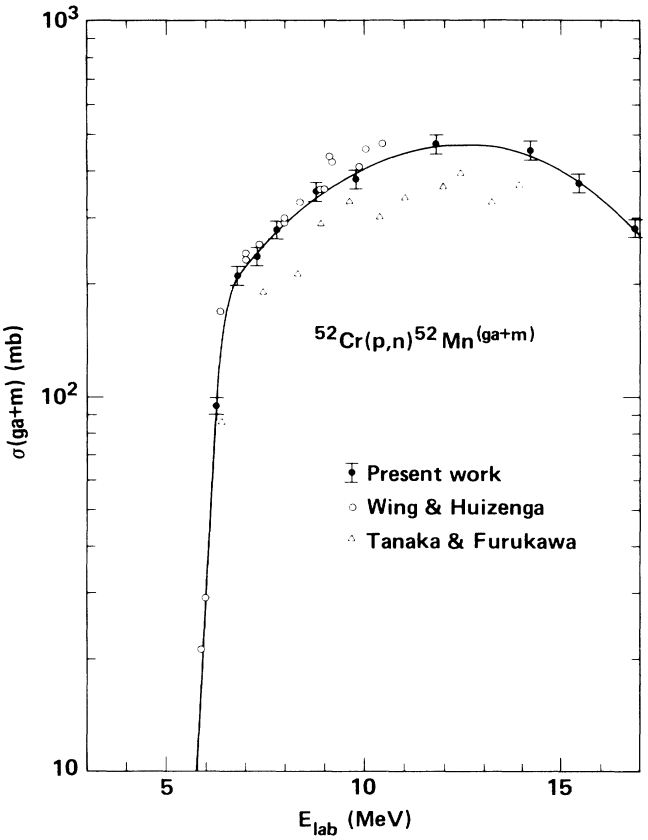

FIG. 4. The $\sigma(ga+m)$ cross section for $^{52}Cr(p,n)^{52}Mn$. Note the comments in the caption of Fig. 3. The contribution from the (p,2n) reaction (threshold at 13.69 MeV) is negligible for these energies. Although the scatter in the data of Tanaka and Furukawa (Ref. 4) is only ±10%, they quote an absolute accuracy of but ±30%.

Boehm *et al.*[1] have made detailed studies near threshold. We have taken data from their Fig. 3 and plotted it on our Fig. 3. The data provide a good extension of our data towards threshold; however, we need to shift their energy scale somewhat to obtain a good overlap with our data, in particular when comparing $\sigma(m)/\sigma(g)$. We find that their lowest energy points yield an experimental threshold which is 50 keV lower than that expected from mass tables. We can bring their data into good agreement with ours by raising their energies by 100 keV. Considering that their measurements were made using a cyclotron and considering possible errors in the values of dE/dx then in use, such an error in energy seems reasonable. (However, the data are plotted in Fig. 3 without correction.) Surprisingly, no decay scheme correction appears needed, nor could it be made easily since the radiation detection was done with a geiger counter. Boehm (private communication) considers our suggested adjustments to their data to be quite reasonable.

Linder and James[2] have also studied the $^{52}Cr(p,n)^{52}Mn^{g,m}$ reactions. However, their data are only qualitatively in agreement with the other data, differing by as much as a factor of 2, and are not shown. Adjusting their β^+ intensity of 35% to the presently accepted value of 28%, does not help.

Tanaka and Furukawa[4] have reported values of $\sigma(ga+m)$. They used scintillation counters with an integral threshold of 0.6 MeV, thus excluding the annihilation radiation. No major corrections for decay-scheme errors seem needed. Their data are plotted in Fig. 4 and compared with results derived from our measurements and those of Wings and Huizenga. Their data are ~30% lower, but consistent with the error limits of ±30% assigned by the authors.

Combining our $^{52}Cr(p,n)^{52}Mn^{g,m}$ data with those of Wing and Huizenga and Boehm *et al.*, the excitation function would seem well established. There are a few points in the data of Wing and Huizenga which clearly should be eliminated, and we believe that the energies of the data of Boehm *et al.* should be raised ~100 keV; otherwise the agreement is good.

Cogneau *et al.*[6] have measured $^{52}Cr(d,2n)^{52}Mn^{g,m}$ from 8.6 to 11.7 MeV (see data comparisons in Figs. 5 and 6). They did β^+ counting assuming a 35% decay intensity.

TABLE II. The $^{52}Cr(d,2n)^{52}Mn^{g,m}$ excitation function.

E_{lab} (MeV)	$\sigma(ga)$[a] (mb)	$\sigma(g)$[b] (mb)	$\sigma(m)$ (mb)
8.17	0.176±0.007		
8.27	0.508±0.020		
8.37	0.961±0.020		
8.46	1.84		0.063±0.010
8.56	2.48		0.199±0.016
8.71	4.71	4.70	0.772
8.97	7.99	7.95	2.45
9.46	17.29	17.11	10.50
9.60	25.03	24.73	17.10
9.89	31.30	30.9	
9.97	34.15	33.70	25.55
10.62	58.34	57.49	48.17
10.97	74.61	73.49	63.85
11.47	87.42	86.04	78.42
11.75	100.6	99.0	90.93
11.76	97.5	95.9	
13.47	141.3	138.9	
13.78	150.1	147.5	146.4
15.05	169.8	166.9	
15.82	177.2	174.2	172.8
15.89	181.6	178.5	
16.91	187.0	183.9	
17.66	192.9	189.6	
17.80	197.2	194.1	177.8
18.25	198.5	195.4	
18.83	198.3	195.2	174.2
19.32	195.5	192.6	
19.58	197.0	194.1	
19.82	197.6	194.7	163.9

[a]These measurements are σ(natural)/abundance of ^{52}Cr (0.8379). Except where noted, the relative accuracy is ±2%; the absolute accuracy is ±3%. Note that this is the apparent cross section (see text).

[b]The cross section was corrected for decay from the isomeric state.

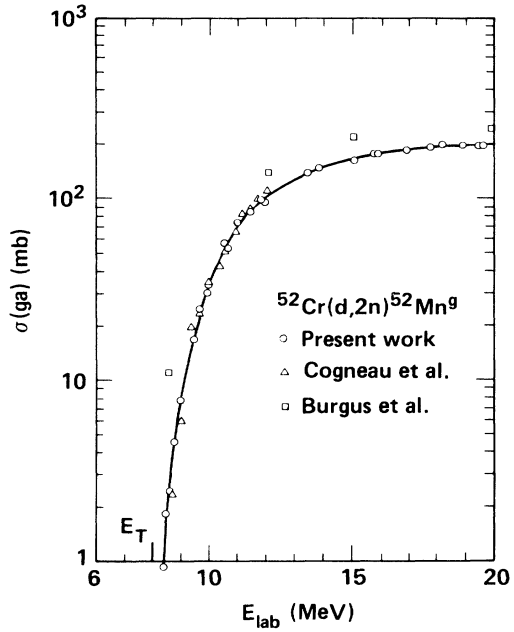

FIG. 5. The $\sigma(ga)$ cross sections for ^{52}Cr(d,2n)^{52}Mn. Note that $\sigma(ga)$ is the apparent ground state cross section (see Sec. III A). Earlier data are shown for comparison. See text for estimates of uncertainties in the earlier data and discussion.

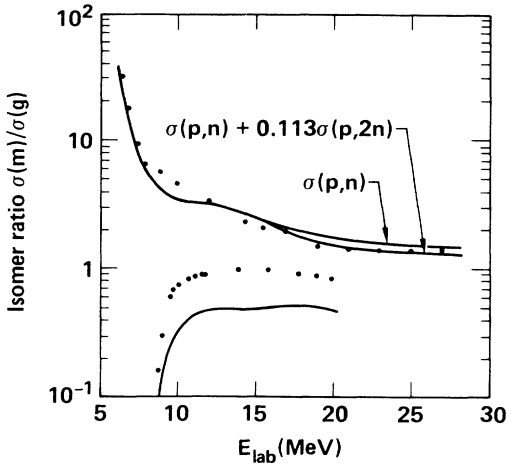

FIG. 7. The isomer ratio $\sigma(m)/\sigma(g)$ for both $^{52+x}$Cr(p,n + xn)^{52}Mn^{g,m} and ^{52}Cr(d,2n)^{52}Mn^{g,m}. Note that the true $\sigma(g)$ is used (see Sec. III A). The solid curves are the results of the calculations $K=380$ MeV^3, 2p-1h for protons and $K=200$ MeV^3, 2p-1h for deuterons). The (p,n) results fit well, but there is a serious discrepancy for the (d,2n) results which is unresolved within the framework of the statistical model as used here.

Correcting their data by 35/28 to allow for the 28% accepted value of β^+ intensity gives apparent ground state cross sections in very good agreement with ours, which is consistent with the uncertainty of 5—10% they place on their data. However, their ^{52}Mn^m data are ~30% lower than our results. Their data are reported in terms of ratios of cross sections to that obtained at 12 MeV. For the ^{52}Mn^m data, there is a jog in the variation with energy just below 12 MeV which makes the normalization suspect. Burgus *et al.*[5] made measurements of ^{52}Cr(d,2n)^{52}Mn^g. We took data from their Fig. 1. They did beta counting assuming a 35% branch, for which we have made the intensity correction 35/28. Their low-energy point at ~8.5 MeV is a factor of 10 larger than our result. They give three other points that are ~30% larger than ours. From the error bars of 5—10% they give for their data, we would expect better agreement.

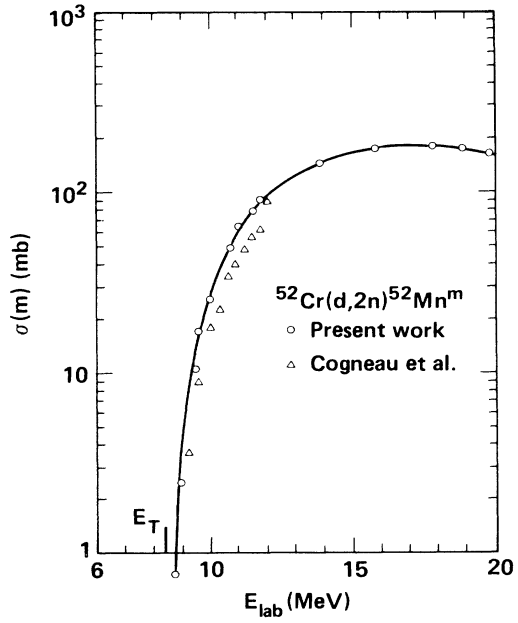

FIG. 6. The $\sigma(m)$ cross sections for ^{52}Cr(d,2n)^{52}Mn. Earlier data are shown for comparison. See text for discussion.

It is only with the ^{52}Cr(d,2n)^{52}Mn^m data that large discrepancies show between our results and data in the literature. We feel that in view of our experimental methods and the good agreement between our data and other data in the literature for the (p,n) reaction, we can make a strong case that ours are the correct results within the stated errors.

IV. THEORETICAL MODELING

The cross sections and isomer ratios were calculated by using the current Livermore version of the STAPRE code[7] of Ströhmaier and Uhl, designed to calculate energy-average cross sections for particle-induced reactions. The reaction is assumed to proceed by, first, preequilibrium particle emission via the exciton model,[14,15] followed by the evaporation of equilibrium particles and γ rays. The latter are treated by the Hauser-Feshbach formalism with angular momentum and parity conservation,[16,17] and width fluctuation correction.[18] (Note that the exciton model does not include angular momentum.) The various physics inputs used for STAPRE were as follows.

(1) Optical model potentials: The optical model potentials were used to generate particle transmission coeffi-

cients. For lack of any specifically suitable potentials for ^{52}Cr, we used global potentials. We used the Moldauer potential[19] for neutrons below 1 MeV and the Rapaport potential[20] above 1 MeV. For protons we used the global potential of Perey[21] and for alpha particles the McFadden-Satchler potential.[22] The deuteron potential is poorly known, so we tried five different potentials. For the results reported here we used the potentials from Löhr and Haeberli[23] below 13 MeV and Perey and Perey above 13 MeV.[24] We also performed calculations with the neutron and proton potentials of Becchetti and Greenlees[25] and the deuteron potentials of Hinterberger *et al.*,[26] Perrin *et al.*,[27] and Daehnick *et al.*[28,29] For the (p,n) reaction we found that the sensitivity of the total (p,n) cross section to the different optical potentials ranged from 5% to 15%, while the sensitivity of the isomer ratio ranged from 2% to 13%. However, the total cross section and isomer ratio for the (d,2n) reaction are quite insensitive to the choice of the potentials. The sensitivity to the deuteron potential is within 4%, and sensitivity to the neutron and proton potentials is about 3%. Our choice of the optical potentials is based, therefore, on a newer evaluation for neutrons by Rapaport,[20] a historically successful proton potential of Perey,[21] and an arbitrary choice for the deuteron potentials[23,24] and the alpha potential.[22]

(2) Level densities: We used the composite nuclear-level-density formalism of Gilbert and Cameron with shell and pairing corrections.[30] The level densities at lower energies were given by a constant-temperature formula, and for higher energies the Fermi gas model was used. These two formalisms were matched at a chosen energy. The model parameters were adjusted to known low-energy discrete levels.[10,31] We included up to 33 low-energy levels in ^{52}Mn (Table III).

(3) Gamma ray strengths: The strengths were taken from Gardner.[32]

(4) Nuclear masses and separation energies: These were taken from the atomic mass table of Wapstra and Bos.[33]

(5) Preequilibrium (PE) models: The transition rates were calculated by the formulas of Williams,[34] corrected for the Pauli principle by Cline.[35] The average residual two-body matrix element that appears in the rate expressions, which determine the transition to equilibrium, was chosen to be[36]

$$|M|^2 = KA^{-3}E^{-1} ,$$

where A is the mass number and E is the excitation energy of the composite system. The quantity K is a constant with the dimension of MeV.[3] Two other parameters were needed in the PE calculations: the initial exciton configuration, i.e., initial particles and holes, and the single-particle level density, $g=(6/\pi^2)a$, where a is the level-density parameter. We treated the parameter K and the choice of initial exciton configurations as free parameters. There are newer PE models in the literature. Our choice of the exciton model is based on convenience. However, note that we also performed calculations with the ALICE code,[13] which contains many of the recent refinements in the PE model. The calculations with ALICE also give fits to the total cross section data similar to those we obtained with the STAPRE code. Since ALICE is based on the Weisskopf-Ewing formalism,[37] it does not conserve angular momentum and therefore cannot be used for isomer-ratio calculations.

TABLE III. Energy levels in ^{52}Mn used in the STAPRE calculation.

E (keV)	J^π	Level branching ratios (%)
0	6^+	beta decays
378	2^+	beta decays
546	1^+	378(100)
732	4^+	0(91) 378(9)
825	3^+	378(100)
870	7^+	0(100)
884	3^+	378(97) 732(3)
887	2^+	378(90) 546(10)
1232	3^+	378(61) 732(27) 887(12)
1254	5^+	0(81) 732(19)
1279	4^+	825(60) 884(40)
1684	5^+	0(69) 732(21) 1279(10)
1955	6^+	0(100)
2044	4^+	825(100)
2130	3^+	378(50) 732(50)
2240	7^+	0(50) 870(50)
2253	4^+	732(50) 825(50)
2261	2^+	378(50) 546(50)
2285	8^+	0(4) 870(96)
2337	3^+	825(51) 887(49)
2631	1^+	546(100)
2667	2^+	378(50) 546(50)
2711	5^+	0(90) 732(10)
2787	3^+	378(60) 546(30) 732(10)
2796	1^+	378(50) 546(50)
2908	9^+	870(29) 2285(71)
2925	0^+	546(100)
2973	6^+	0(80) 870(20)
3022	4^+	1684(80) 732(20)
3080	5^-	732(100)
3097	3^+	1684(80) 732(20)
3106	2^+	546(70) 2130(30)
3200	6^+	0(40) 1684(60)

A. Modeling results

Figure 8 shows the total cross section for the $^{52+x}$Cr(p,n + xn) reactions compared with results of our calculations for σ(p,n) and for σ(p,n) + 0.113σ(p,2n) (the factor 0.113 is the isotopic ratio of ^{53}Cr/^{52}Cr). K in the PE model was 380 MeV[3] (see Ref. 38) and the initial exciton configuration was 2p-1h. The fit to the data is sensitive to the PE model only above 15 MeV. The results for σ(p,n) and σ(p,n) + 0.113σ(p,2n) are shown separately. The lower curves show the results for the compound effects that would prevail in the absence of the PE process. Thus we note the dominant contribution of PE emission in this region. Also shown is the total cross section alone for 0.113σ(p,2n). In the course of the calculations we used a wide variation in K and initial exciton configuration, but we could not improve over the parameters of the Milano group.[38]

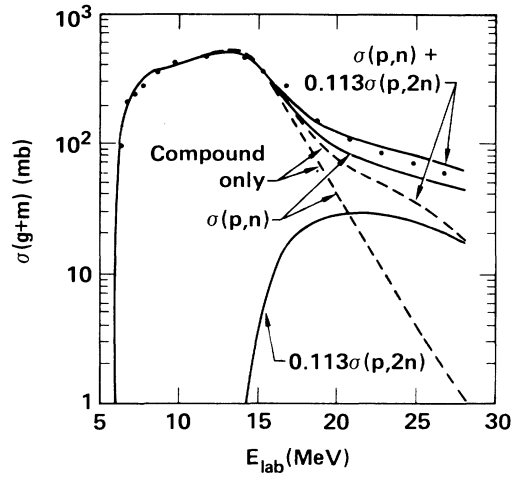

FIG. 8. The $^{52+x}$Cr(p,n + xn)^{52}Mn data compared with calculation. The results above 15 MeV reflect the contribution (0.113) from the ^{53}Cr(p,2n) reaction normalized to the abundance of ^{52}Cr. The bottom curve shows 0.113σ(p,2n) alone. Also, above 15 MeV we note the effects of the parameters in the PE model ($K=380$ MeV^3, 2p-1h; solid curves equal total cross sections and dashed curves equal compound alone.

Figure 7 shows our attempt at calculating the isomer ratio for both the (p,n) and (d,2n) data. The (p,n) calculations use $K=380$ MeV^3 and a 2p-1h initial exciton configuration, and the (d,2n) results use $K=200$ MeV^3 and a 2p-1h initial exciton configuration. The fit to the (p,n) data is remarkable. The deviation at 8—10 MeV is a region of overlap of two calculations (optical model changes) and may not be significant.

Figure 9 shows the cross sections for $\sigma(g+m)$ for the (d,2n) reaction compared with calculations at $K=200$ MeV^3 using various initial exciton configurations. The results are not strongly sensitive to values of K. For $K=380$ MeV^3 and 3p-1h, the results are higher by 1—6%; for 2p-1h, the results are higher by 2—10%; and for 2p-0h, they are 10—22% higher.

One can bring the total cross section fairly close to experiment with a 2p-0h initial exciton configuration. But this improvement does not improve the fit to the isomer ratio (see Fig. 7). However, earlier work by Bisplinghoff *et al.*[39] and Kleinfeller *et al.*[40] indicates that 3p-1h or 2p-1h may be a better choice for the initial exciton configuration. Since our choice is coupled with the parameter K, it is not possible for us to make a definitive judgement on the choice of the initial exciton configuration. However, our results suggest that a reasonable choice lies between 2p-0h and 3p-1h. Although we had good success in modeling the total cross section for the (p,n) reaction, for the (d,2n) data the calculations would appear to be too high by about 50%.

Figure 10 shows further details of the isomer ratio calculations for the (d,2n) reaction. As in Fig. 9, the results of various PE configurations are explored. Note that the calculated isomer ratios for 3p-1h are very close to those for 2p-1h. Although the total cross section is sensitive to the choice of initial exciton numbers, such is not the case for the isomer ratio. The PE model as used here does not help us to remove the discrepancy in the (d,2n) isomer ratio.

Figure 11 shows the effect of varying exciton configurations on the PE fraction σ_{PE}/σ_R for both proton and deuteron reactions on ^{52}Cr. The quantity σ_{PE} is the total PE cross section for the emission of n, p, d, and α, and σ_R is the total optical model reaction cross section. Thus $\sigma_R-\sigma_{PE}$ is the total cross section for the formation of a compound nucleus formed by complete fusion of target and projectile. The results show relative competition between PE and compound processes and show the relative fractions needed to fit the experimental data. The larger PE fraction for the deuteron-induced reaction relative to the proton-induced reaction is partly a consequence of the larger excitation energy of the composite system for a chosen bombarding energy. However, the large PE fraction for 2p-0h for the (d,2n) reaction appears unrealistic.

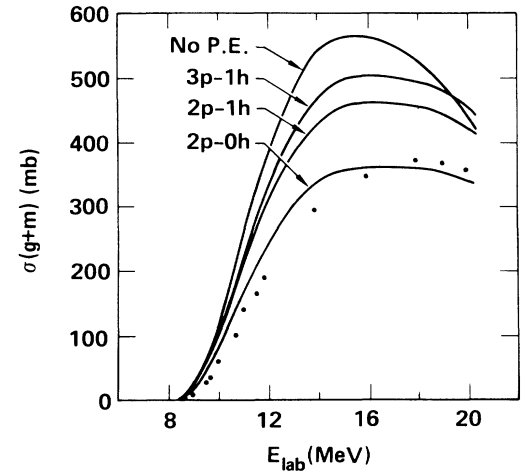

FIG. 9. The ^{52}Cr(d,2n)^{52}Mn data compared with calculation. K was held constant at 200 MeV^3 and the initial exciton configuration was varied. Although 2p-0h fits the data approximately, it is considered quite improbable (see text); also note Fig. 11.

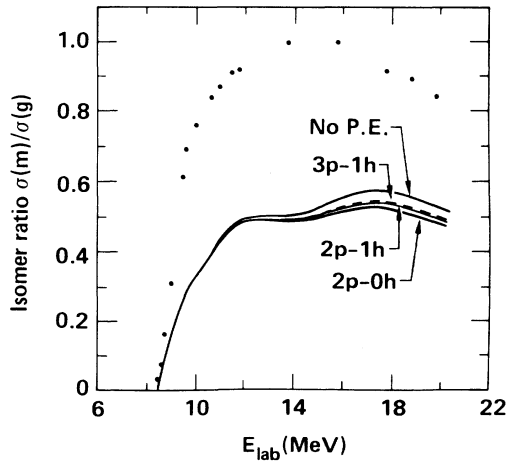

FIG. 10. The isomer ratio for the ^{52}Cr(d,2n)^{52}Mn reaction compared with calculations using $K=200$ MeV^3 and for different initial exciton configurations.

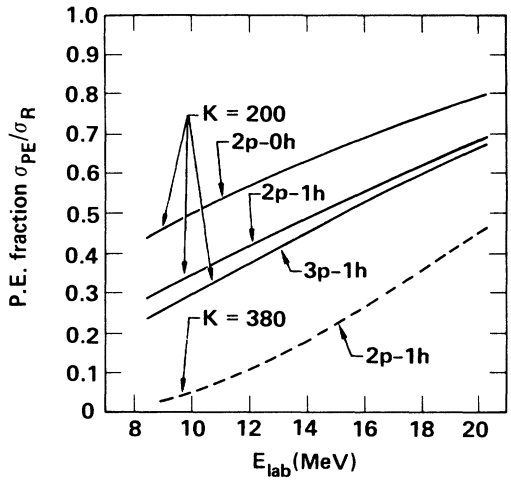

FIG. 11. Preequilibrium fractions for deuteron induced reaction ($K = 200$ MeV^3 and different initial exciton configurations) and for proton induced reaction ($K = 380$ MeV^3 and 2p-1h initial exciton configuration).

We emphasize that we consider both the initial exciton configuration and the quantity K as strictly free parameters. Although in the companion paper we took 2p-1h results as the standard statistical model, our conclusions there would not be affected by the choice of 3p-1h, but would be affected by the 2p-0h configuration. What is shown in Figs. 9 and 10 is the sensitivity of our calculation with respect to the PE fraction rather than the initial configuration alone (see Fig. 11). The important result is that the isomer ratios are independent of PE fractions. Angular momentum effects may be partly responsible for this result (see next section for further comments on this).

V. DISCUSSION AND CONCLUSIONS

We have made measurements on the $^{52+x}$Cr(p,n, + xn) and ^{52}Cr(d,2n) cross sections for the production of ^{52}Mn^{g,m} from targets of natural chromium. We note that only above about 15 MeV is the (p,2n) reaction significant in the proton data. Rather detailed calculations were made using the STAPRE code based on the Hauser-Feshbach formalism and the exciton PE model. Using reasonable parameters for the PE model, we were able to reproduce the (p,n) data, $\sigma(g+m)$ and $\sigma(m)/\sigma(g)$, quite convincingly. Applying the same treatment to the deuteron data met with little success. Although it was possible to produce $\sigma(g+m)$ by adjusting the initial exciton configuration, no variation of the PE model parameters would reproduce the isomer ratio.

To look for possible reasons for this effect, we examine the steps in the calculation. The most sensitive parts of the calculation are the choice of the level densities, ^{52}Mn energy levels, and associated γ-ray branching ratio and PE configuration. In contrast, the results are not particularly sensitive to the level data used for the initial compound nucleus and for other nuclei involved in the decay process, except for ^{52}Mn. As additional support of this, we note that the ALICE code[13] (which does not include discrete levels) gives results similar to those of the STAPRE code[7] for the total cross section. Of course, ALICE cannot be used to calculate isomer ratios.

The isomer ratios are extremely sensitive to energy-level data for ^{52}Mn for a few MeV of excitations, especially the γ-ray branching ratios. The remarkable success of the calculations at reproducing the (p,n) data argues strongly that the various inputs were acceptable: specifically, we identify the level data (Table III) and level densities of ^{52}Mn, the level densities of ^{52}Cr, the proton and neutron optical potentials, and the choice of PE model parameters.

The choices available for explaining the (d,2n) data are very much reduced by the proton results. Adjustments of level densities of ^{53}Mn and ^{53}Cr could bring the total (d,2n) cross section to agree with the data, without affecting the (p,n) results. This, however, will not improve the isomer ratio. In principle, we can fit the (d,2n) isomer data by changing the ^{52}Mn branching ratios, but that would destroy the excellent (p,n) results and is not admissible. To explain the (d,2n) data, we must look at the early steps in the reaction. We examine the PE model further.

There are many uncertainties in the PE model and we showed in Fig. 10 that the adjustments of PE model parameters could explain the isomer ratio. The PE model, however, as used here, does not include angular momentum. Hence, we have assumed that the spin distribution of the PE components would be the same as that for the equilibrium Hauser-Feshbach result. This may be a poor approximation, and it would be interesting to see what effect a more realistic model would have.

The cause of the problem in explaining the deuteron data, we believe, is due to the appreciable probability that the loosely bound deuteron breaks up in the entrance channel (e.g., see the work of Pampus *et al.*[41]), thus significantly changing the entrance-channel spin distribution. In effect, then, we have a part that goes by (d,2n) reaction and a part that goes by deuteron breakup with subsequent capture by the nucleus of a low-partial-wave proton in a more or less direct reaction. These breakup fusion effects are considered in a companion paper, yielding a very marked improvement over the statistical model alone.[42]

ACKNOWLEDGMENTS

We thank the Materials Fabrication Division of LLNL for making the targets, the Cyclograaff crew for making the irradiations, and R. Anderson for help in gamma counting. R. Nagle rechecked the half-life of ^{52}Mn^m for us. R. Meyer put together the ^{52}Mn energy-level data for us and we acknowledge several discussions on nuclear structure with him. We acknowledge helpful discussions with D. Gardner and M. Gardner about the STAPRE code. We acknowledge many discussions with M. Blann and T. Tamura, especially the former regarding the PE model and the ALICE code. Discussions with E. D. Arthur of Los Alamos National Laboratory on many aspects of the statistical model calculations are also acknowledged. This work was performed under the auspices of the U.S. Department of Energy at the Lawrence Livermore National Laboratory under Contract No. W-7405-ENG-48.

[1]F. Boehm, P. Marmier, and P. Preiswerk, Helv. Phys. Acta **25**, 599 (1952).
[2]B. Linder and R. A. James, Phys. Rev. **114**, 322 (1959).
[3]J. Wing and J. R. Huizenga, Phys. Rev. **128**, 280 (1962).
[4]S. Tanaka and M. Furukawa, J. Phys. Soc. Jpn. **14**, 1269 (1969).
[5]W. H. Burgus, G. A. Cowan, J. W. Hadley, W. Hess, T. Shull, M. L. Stevenson, and H. F. York, Phys. Rev. **95**, 750 (1954).
[6]M. Cogneau, L. Gilly, and J. Cara, Nucl. Phys. **79**, 203 (1966).
[7]D. G. Gardner, Livermore version of a statistical model code originally written by B. Ströhmaier and M. Uhl, Institut für Radiumforschung and Kernphysik (Vienna), Report No. IRK-76/01 with Addenda, 1976.
[8]M. G. Mustafa, H. I. West, Jr., R. G. Lanier, and T. Tamura, Bull. Am. Phys. Soc. **17**, 33 (1986).
[9]R. Colle, R. Kishore, and J. B. Cumming, Phys. Rev. C **9**, 1819 (1974).
[10]C. M. Lederer, V. S. Shirley, E. Browne, J. N. Dairiki, R. E. Doebler, A. A. Shihab-Eldin, L. J. Jardine, J. K. Tuli, and A. B. Buyrn, *Table of Isotopes,* 7th ed. (Wiley, New York, 1978).
[11]R. Gunnink, private communication.
[12]R. Gunnink and J. B. Niday, Lawrence Livermore National Laboratory Report UCRL-51061, 1972.
[13]M. Blann, private communication.
[14]J. J. Griffin, Phys. Rev. Lett. **17**, 478 (1966).
[15]M. Blann, Annu. Rev. Nucl. Sci. **25**, 123 (1975).
[16]W. Hauser and H. Feshbach, Phys. Rev. **87**, 336 (1952).
[17]E. Vogt, Adv. Nucl. Phys. **1**, 261 (1968).
[18]P. A. Moldauer, Rev. Mod. Phys. **36**, 1079 (1964).
[19]P. A. Moldauer, Nucl. Phys. **47**, 65 (1963).
[20]J. Rappaport, Phys. Rep. **87**, 25 (1982).
[21]F. G. Perey, Phys. Rev. **131**, 745 (1963).
[22]L. McFadden and G. R. Satchler, Nucl. Phys. **84**, 177 (1966).
[23]J. M. Löhr and W. Haeberli, Nucl. Phys. **A232**, 381 (1974).
[24]C. M. Perey and F. G. Perey, Phys. Rev. **132**, 755 (1963).
[25]F. D. Becchetti, Jr. and G. W. Greenlees, Phys. Rev. **182**, 1190 (1969).
[26]F. Hinterberger, G. Mairle, U. Schmidt-Rhor, and G. J. Wagner, Nucl. Phys. **A111**, 265 (1968).
[27]G. Perrin, Nguyen Van Sen, J. Arvieux, R. Darves-Blane, J. L. Durand, A. Fior, J. C. Gondrand, F. Merchez, and C. Perrin, Nucl. Phys. **A282**, 221 (1977).
[28]W. W. Daehnick, J. D. Childs, and Z. Vrcelj, Phys. Rev. C **21**, 2253 (1980) (potential 79 DCV,L).
[29]W. W. Daehnick, private communication.
[30]A. Gilbert and A. G. W. Cameron, Can. J. Phys. **43**, 1446 (1965).
[31]R. A. Meyer, private communication.
[32]D. G. Gardner, *Neutron Radiative Capture,* Vol. 3 of *Neutron Physics and Nuclear Data in Science and Technology,* edited by R. E. Chrien (Pergamon, New York, 1984), p. 62.
[33]A. H. Wapstra and K. Bos, At. Data Nucl. Data Tables **19**, 175 (1977).
[34]F. C. Williams, Jr., Nucl. Phys. **A166**, 231 (1971).
[35]C. K. Cline, Nucl. Phys. **A195**, 353 (1972).
[36]C. Kalbach-Cline, Nucl. Phys. **A210**, 590 (1973).
[37]V. F. Weisskopf and D. H. Ewing, Phys. Rev. **57**, 472 (1940).
[38]G. M. Braga-Marcazzan, E. Gadioli-Erba, L. Millazzo-Colli, and P. G. Sona, Phys. Rev. C **6**, 1398 (1972).
[39]J. Bisplinghoff, J. Ernst, R. Löhr, T. Mayer-Kuckuk, and P. Meyer, Nucl. Phys. **A269**, 147 (1976).
[40]J. Kleinfeller, J. Bisplinghoff, J. Ernst, T. Mayer-Kuckuk, G. Bauer, B. Hoffmann, R. Shyam, F. Rösel, and D. Trautmann, Nucl. Phys. **A370**, 205 (1981).
[41]J. Pampus, J. Bisplinghoff, J. Ernst, T. Mayer-Kuckuk, J. Rama Rao, G. Bauer, F. Rösel, and D. Trautmann, Nucl. Phys. **A311**, 141 (1978).
[42]M. G. Mustafa, T. Tamura, and T. Udagawa, following paper, Phys. Rev. C **35**, 2077 (1987).